Cyanobacteria That Produce Megamolecules with Efficient Self-Orientations

Maiko K. Okajima,[†] Daisaku Kaneko,[†] Tetsu Mitsumata,[‡] Tatsuo Kaneko,*[,†] and Junji Watanabe[§]

School of Materials Science, Japan Advanced Institute of Science and Technology, 1-1 Asahidai, Nomi, Ishikawa 923-1292, Japan, Department of Polymer Science and Engineering, Faculty of Engineering, Yamagata University, 4-3-16 Jonan, Yonezawa 992-8510, Japan, and Graduate School of Science and Engineering, Tokyo Institute of Technology, 2-12-1 Ookayama, Meguro-ku, Tokyo 152-8550, Japan

Received December 19, 2008; Revised Manuscript Received February 4, 2009

ABSTRACT: Liquid crystallization of structural megamolecules in plants is very significant in understanding of biopolymer self-orientation and developing plant-derived functional materials. Cyanobacterial megamolecules, sacrans (molecular weight: 1.6×10^7 g/mol), are polysaccharides derived from the extracellular matrix of *Aphanothece sacrum*, and are observed as self-orienting micro rods longer than 3 μm in dilute solution at $c =$ 0.01 wt % by optical microscopes. Sacran chains form double helixes at $c > 0.09$ wt % and form huge domains (centimeter scale) of liquid crystals at $c > 0.5$ wt % which is quite low when compared to conventional liquid crystalline polysaccharides. Mesogenic helical chains of sacrans have extremely high aspect ratios of 1600 for highly persistent lengths of 32 μm.

Introduction

Investigations with lyotropic liquid crystalline (LC) properties of megamolecules whose lengths are high enough to allow for optical observations (molecular weight, M_w, over 10^7 g/mol) have a potential significance in self-orientation of biological materials as well as in material sciences. Most plants contain giant polysaccharides, celluloses, whose derivatives are widely studied as LC polymers[1−4] and LC structures in plant cell walls are composed mainly of cellulose fibers with high degrees of orientation, which may play a role in supporting plant bodies.[5,6] However intact celluloses with high M_w can hardly be extracted because of (their inherent) insolubility. DNAs which have M_w higher than 10^7 g/mol as cited in the literature, adopt LC structures for efficient storage in chromosomes, [7] and the M_w of DNA is remarkably reduced to a scale of 10^6 g/mol during extraction processes.[8] Thus LC behaviors of megamolecules have never been reported despite their high potential. We previously reported the successful extraction of novel supergiant macromolecules "sacrans" (M_w: 1.6×10^7 g/mol) from the jelly extracellular matrix, ECM, of *Aphanothece sacrum*[9,10] a species of cyanobacteria which are very simple organisms and have often been regarded as excellent plant models in terms of structural biology and photosynthetic science.[11] The extracted yield of sacran was 70−80 wt % in dried materials of *A. sacrum*, indicating that the main component of *A. sacrum* ECMs might be sacran. Transmission electron and atomic force microscopic studies of sacran illustrated that the length of sacran chains attained 8 μm. Differently from celluloses, sacrans are heteropolysaccharides composed of various sugar residues such as Glc, Gal, Man, Xyl, Rha, Fuc, GalA (anionic), and GlcA (anionic), with a composition of 25.9: 11.0: 10.0: 16.2: 10.2: 6.9: 4.0: and 4.2, and contain trace amounts (ca. 1.0%) of Ara, GalN (cationic), and Mur (amphoteric). Sacrans are sulfated in 10 mol % to monosaccharide residues. Overall, sacrans are amphoteric megamolecule whose self-organization may strongly affect properties of *A. sacrum* ECMs with discolored regions, which are available atop large colonies living in cultivation rivers, which are opaque-like LC materials. Besides this, we noticed that *A. sacrum* biomaterials are very tough despite high water contents of 97.5−98.3 wt %. These aforementioned findings motivated us to investigate LC behaviors of sacran megamolecules. Here we show that sacran aqueous solutions form huge LC domains under extremely low concentrations and sacran chains form giant mesogens with extremely high aspect ratios.

* Corresponding author. Telephone: +81-761-51-1631. Fax: +81-761-51-1635. E-mail: kaneko@jaist.ac.jp.
[†] School of Materials Science, Japan Advanced Institute of Science and Technology.
[‡] Department of Polymer Science and Engineering, Faculty of Engineering, Yamagata University.
[§] Graduate School of Science and Engineering, Tokyo Institute of Technology.

Results

Sacran was extracted from frozen samples of *A. sacrum* by a previously reported method[10] but cultivation environments such as river water temperature, mineral concentration, season, and effects from other creatures would differ in various *A. sacrum* biomaterials. We worried about the influence from the cultivation environment on sacran structures. However UV−vis and FT-IR/ATR spectra (a representative spectrum: Figure S1) were intrinsically the same in any sacran sample derived from different samples of *A. sacrum* ($n = 10$ picked up from the Kogane river in every season over 2 years), which indicated that basic structure, such as functional groups, was independent of cultivation environments.

Extraction and LC Properties. Figure 1a shows a microscopic photo of sacran fibers in the dry state, taken under the cross-nicol using a first-order retardation plate ($\lambda = 530$ nm) inserted into the light path. The polarized microscopic observation shows oriented fibers with a thickness of less than 10 μm. The fiber birefringence is negative, as evidenced by both subtractive birefringence (blue color) in the fiber lying from the upper left to the lower right and additive birefringence (orange color) in the fiber lying from the upper right to the lower left. The negative birefringence strongly suggests that sacran backbones lie along the fiber axis. X-ray diffraction diagrams of the fibers in dry states showed only a broad halo without crystalline peaks, indicating sacran fibers were noncrystalline, presumably due to many kinds of sugar residues.[10] The dry fibers easily dissolved in hot water to create very viscous and translucent solution. Figure 1b shows crossed-polarizing mi-

10.1021/ma802829x CCC: $40.75
Published on Web 03/03/2009

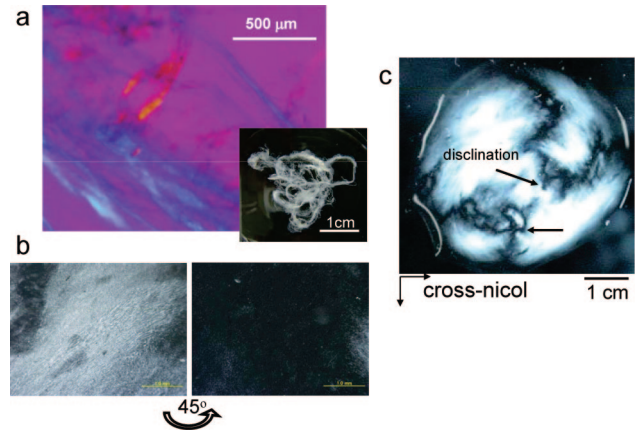

Figure 1. Optical images of sacran materials. (a) Crossed-polarizing microscopic photos of dried fibers with a first-order retardation plate ($\lambda = 530$ nm). Inset: Macroscopic view of the fibers dispersed in 2-propanol. (b) Crossed-polarizing microscopic images of sacran aqueous solution with 0.5 wt % concentrations. Left: bright region. Right: bright region darkened upon a 45° rotation. (c) Bright macroscopic domain and Schlieren texture (arrows) of sacran aqueous solution with 0.5 wt % concentrations taken under cross-nicol polarimetry.

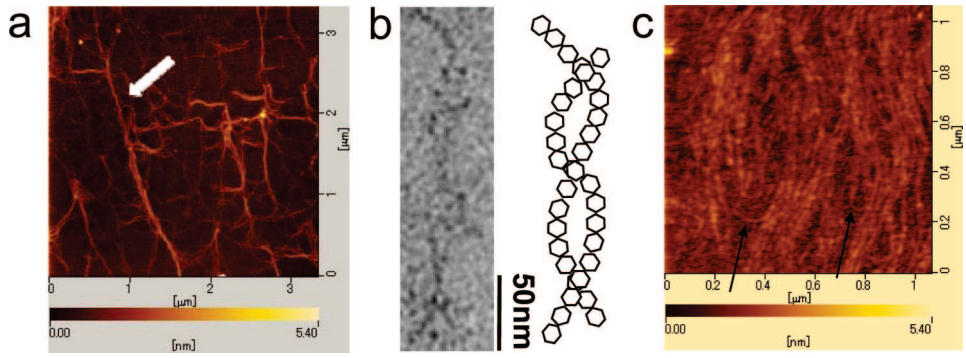

Figure 2. Microscopic images of sacran chains. (a) Atomic force microscopic (AFM) images of sacran chains dried from very dilute solutions on mica substrates (arrow: a representative bundle of sacran chains). (b) Transmission electron microscopic (TEM) images of specimens dried on a carbon-coated Cu grid. Illustration: helical form of sacran chains speculated as the basis of TEM images. (c) AFM images of sacran chains dried from more concentrated solutions than the solution in Figure 3a. Arrows show sacran chains bridging sacran ropes.

croscopic photos of sacran solutions with a concentration of 0.5 wt %. The bright region contains many sacran rods lining up but darkened by a 45° (or 135°) rotation for lines to be parallel with a polarizer (or analyzer) axis. The aforementioned phenomenon is characteristic of self-orientation. X-ray diffraction diagrams of microfibers in aqueous solutions showed only a broad halo without crystalline peaks, indicating microfibers were still noncrystalline. The birefringence in the solution is generally caused by crystalline particle dispersions or the molecular orientation of solutes. In the present case, X-ray studies did not confirm crystalline particles. Figure 1c shows the image of the sacran aqueous solution with a concentration of 0.5 wt % (3 mL) put on a glass dish with a round-bottom. The solution was irradiated (brightly) by the white backlight under crossed-polarizers, to show a birefringence and continuous brushes around point defects with a disclination of $s = \pm^1/_2$ (arrows). These textures including brushes, so-called Schlieren textures, indicate that sacran chains form the nematic LC phase.[12] We can speculate that the LC phase may be attributed to a special form of sacran, as a microbial polysaccharide, schizophyllan, which forms a rigid triple helix to show an LC phase.[13] It was noticeable that the domain surrounded by brushes was very big (millimeter to several centimeter scale) even without any treatment by external forces; i.e., sacran chains automatically aligned in the macroscopic range.

In order to analyze the structure of sacrans in more detail, AFM images of sacran chains dried from solutions with concentrations of 1 ppm on mica substrates were observed. Figure 2a shows sacran chains as whitish lines, indicating a few sacran chains formed bundles with twisted morphologies (a representative bundle is indicated by the arrow; ca. 3 μm length). Close-up images taken by TEM revealed a double helix form of the sacran bundle (Figure 2b), where helixes were loosely wound as shown in the right illustration of Figure 2b, and its thickness and helical pitch are about 20 and 120 nm, respectively. The driving force for the bundle formation is not clear but we can speculate that interchain interactions of sacran may be related with functional groups such as uronic acid, sulfated sugars, and amino sugars, which were all previously detected[10] Helical chains generally behave like rigid rods seen as almost-straight lines and possibly helical chains contributed to exhibit LC phases in sacran solutions. We attempted to catch bundle orientations as AFM images using specimens dried from sacran solution at $c = 0.01$ wt % and obtained Figure 2c where many twisted ropes of sacran chains lined up, suggesting a close relationship between sacran helixes and LC.

Dielectric Behavior. When sacran transform from single chains to double helixes, the ionic environment around sacran chains also changes. In order to investigate the ionic environment of sacran chains under various concentrations, we investigated the dielectric behavior of sacran solutions with changing concentrations. Figure 3a shows dielectric spectra of sacran solutions with various concentrations. We measured the dielectric constant ϵ'_r (relative dielectric constant) of sacran aqueous solutions; we extracted ϵ'_r by removing the electrode polarization component from as-measured data, assuming that the electrode polarization is equal to the dielectric constant of KCl saline

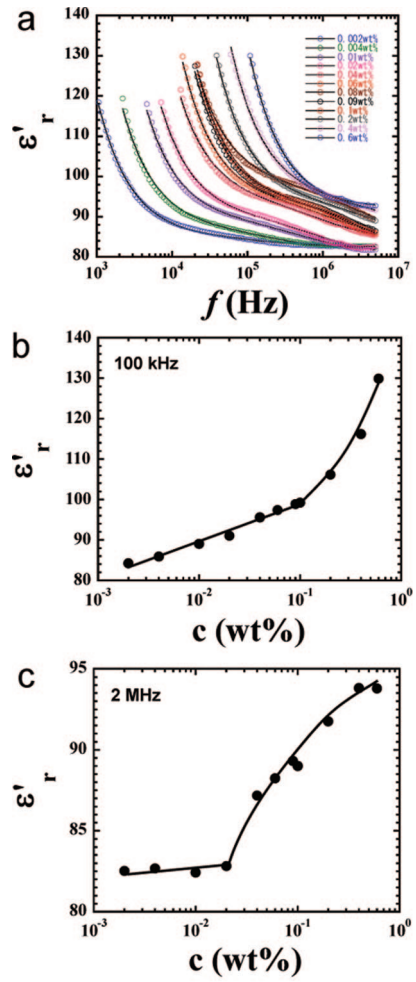

Figure 3. Dielectric constants for sacran aqueous solutions with various concentrations: (a) dielectric spectra, (b) concentration dependence of dielectric constant at 100 kHz, and (c) concentration dependence of dielectric constant at 2 MHz.

solutions with nearly the same electric conductivity as the sample.[14] Large relaxations at low frequencies and a small one at high frequencies were observed in dielectric spectra. Both relaxations were fitted by the following equation consisting of two Debye relaxations:[15]

$$\varepsilon'_{w} + \frac{\Delta\varepsilon_{L}}{2}\left\{1 - \frac{\sinh x_{L}}{\cosh x_{L} + \cos(\pi/2)}\right\} + \frac{\Delta\varepsilon_{H}}{2}\left\{1 - \frac{\sinh x_{H}}{\cosh x_{H} + \cos(\pi/2)}\right\}$$

Where $x_{L,H} = \ln\omega\tau_{L,H}$; ω is the angular frequency of the electric field, $\tau_{L,H}$ is the mean relaxation time of low or high frequency relaxations. ϵ'_{w} is the dielectric constant of pure water ($\epsilon'_{w} = 82$). $\Delta\epsilon'_{L,H}$ is the dielectric increment of low or high relaxations, respectively. It is widely accepted that polyelectrolyte solutions exhibit two dielectric relaxations; one is a low-frequency relaxation in the kHz range and another is a high-frequency relaxation in the MHz range. The low-frequency relaxation arises from fluctuations in bound counterions along the polymer chain. The high-frequency relaxation is due to fluctuations in loosely bound counterions perpendicular to the polymer chain.[16,17] According to the fitted equation, the low-frequency relaxation time of very dilute solutions of $c = 0.002$ wt % were determined to be $\tau = 8.1$ ms. The aforementioned result indicates that the fluctuation length ξ_L of bound counterions along the sacran chain is 4.5 μm using a relation of $\xi_L = \sqrt{2D\tau_L}$; D is the diffusion constant of Na^+ ion in a free medium (1.22×10^{-9} m^2/s). According to the theory of Mandel,[18] the contour length $\sqrt{12}\xi_L$ corresponding to the length of the sacran chain was calculated as 16 μm which is in the same order of the length obtained from AFM (Figure S2), that is, the low-frequency relaxation is due to the counterion fluctuation along sacran chains (Figure 4a,b). Such long τ have been observed in another giant macromolecule, Na−DNA ($\tau = 68$ ms; degree of polymerization 12000),[19] or a polyelectrolyte gel ($0.7 < \tau < 2.1$ ms),[20] suggesting that sacran has a long and electrostatically continuous chain.

Figure 3b shows the dielectric constant at 100 kHz for sacran aqueous solutions under various concentrations. The dielectric constant gradually increased with the sacran concentration but the increasing rate clearly rose at $c = 0.09$ wt %. In addition, the relaxation time of bound counterions along sacran chains suddenly shortened between 0.08−0.09 wt % (Figure S3). Actually, the relaxation time of bound counterions at $c = 0.09$ wt % was determined to be 0.95 ms, which corresponds to a fluctuation length of 1.5 μm. The helical structure of sacran chains might restrict the long fluctuation of bound counterions. We can speculate that some association points of anions and cations might make terminals on fluctuations pass as schematically shown in Figure 4c. Otherwise, the short-time relaxation may be caused by the enhanced mobility of bound counterions because the electrostatic potential valley along the chain is weakened by electrostatic associations of sacran chains.

Figure 3c shows the dielectric constant at 2 MHz for sacran aqueous solutions with various concentrations. The dielectric constant remained constant below 0.02 wt % but suddenly increased at $c = 0.02$ wt %. Since the M_w of sacran is very high, 1.6×10^7, c^*, the critical concentration at which chain overlap occurs, is very low, 0.012 wt % as calculated using the following equation:[21]

$$c^* \approx a^{-3}N^{-4/5},$$

Here a is the length of the monosaccharide (0.65 nm), and N is the number of monosaccharide residues in sacran (8.9×10^4). The calculated c^* agrees with the critical value of 0.02 wt %. We estimated the high-frequency relaxation time using the same procedure for estimating the low-frequency relaxation. High-frequency relaxation times at $c = 0.002$ and 0.09 wt % were estimated to be 1.1 μs and 54 ns, which correspond to fluctuation lengths of 52 and 11 nm, respectively. Loosely bound counterions have short relaxation times and fluctuation lengths at $c > 0.02$ wt %, which originate from the decrease in the correlation length of sacran chains and loosely bound ions fluctuate among chains are shown in Figure 4b.

Rheooptical Behavior. We next investigated viscosities and polarized optical behaviors of sacran solutions under various concentrations in order to determine the critical concentration of liquid crystallization. Figure 5a shows the shear rate dependence of rotation viscosities of sacran solutions with concentrations ranging between 0.06 and 1.5 wt %. Sacran solution viscosities increased upon increasing concentrations. Figure 6a shows zero shear viscosities, which were estimated by extrapolating viscosity data at a shear rate range of 10^{-3}−10^{-2} 1/s plotted against concentration. Zero shear viscosity also showed an increase with concentration but with an inflection point around a concentration of 0.25−0.5 wt %. Since the inflection point may relate with the liquid crystallization of sacran solutions, their polarized optical behaviors were investigated. In order to evaluate the orientation state of sacran chains, the intensity of white light transmitted through sacran solutions under crossed polarizers was measured by a photometry system equipped with a rheometer as illustrated in Figure S4. Figure

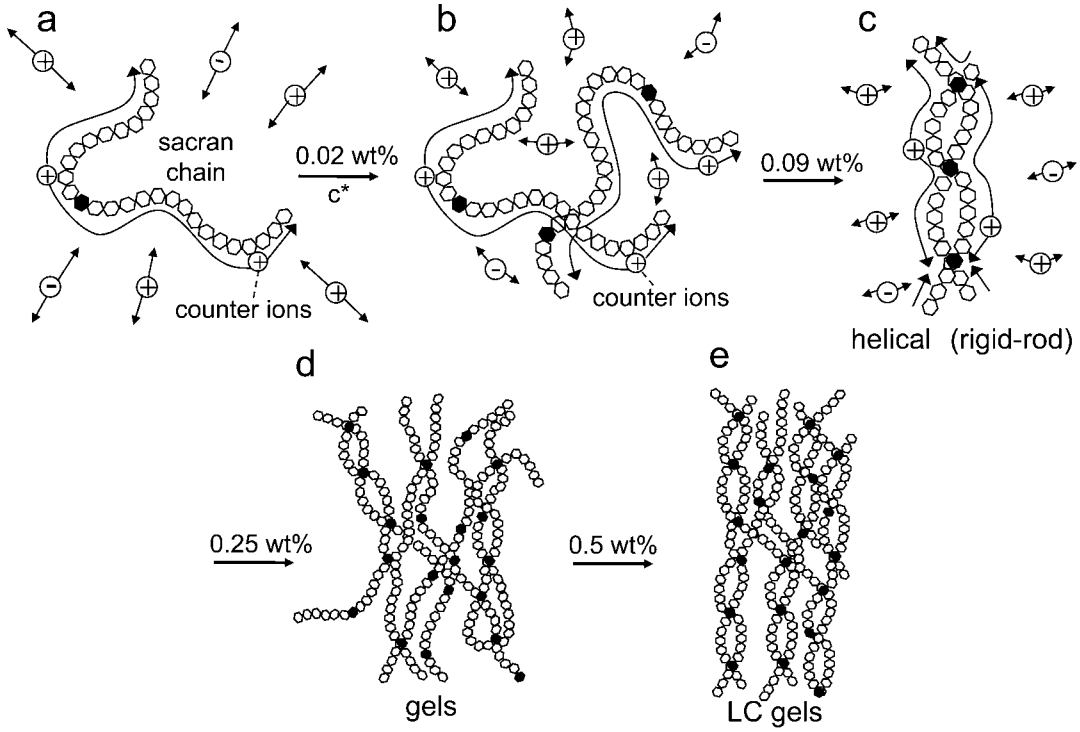

Figure 4. Schematic illustration of sacran self-organization upon a concentration increase. Circled + and − marks refer to counter cations and anions of sacran chains, respectively. Black points on sacran chains refer to moieties containing amino sugar residues. Arrow lengths correspond to fluctuation lengths.

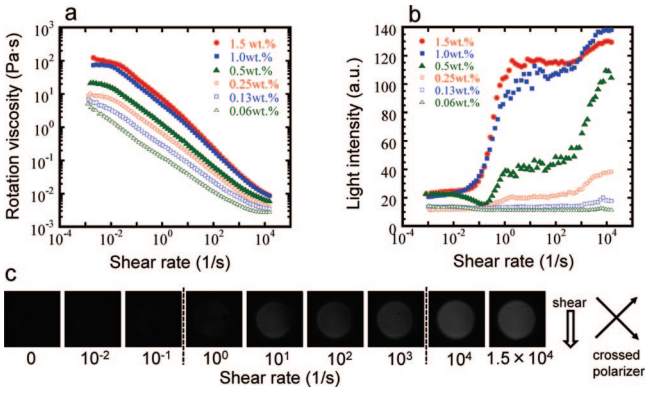

Figure 5. (a) Shear rate dependence of rotation viscosity for sacran solutions with various concentrations. (b) Intensity of white light transmitted through sacran solutions with various concentrations, measured under a crossed polarizer. (c) Crossed-polarizing images of white light transmitted through sacran solutions with a concentration of 0.5 wt %. Dotted lines show critical concentrations in a light-intensity increase.

5b shows the light intensity change as a function of shear rate. Light intensities of sacran solutions with concentrations of 1.5, 1.0 and 0.5 wt % were higher than those of 0.25, 0.13, and 0.06 wt % when shear rates were very low. Then we estimated the zero shear intensity by extrapolating intensity data at a shear rate range of 10^{-3}−10^{-2} 1/s and plotted it against concentrations (Figure 6b). Zero shear intensities of sacran solutions jumped up at concentrations of 0.25−0.5 wt %, indicating that the orientation of sacran chains increased drastically in this concentration range. This result indicates the critical concentration of liquid crystallization of sacran solution lay in 0.25−0.5 wt % where the inflection point appeared in the zero shear viscosity plot (Figure 6a). The sacran solution showed a thixotropic effect; the viscosity of sacran solutions with concentrations of 0.06, 0.13, 0.25, 0.5, 1.0, and 1.5 wt % showed 3.3, 3.8, 4.1, 4.5, 5.5, and 6.4 times decrease, respectively, with

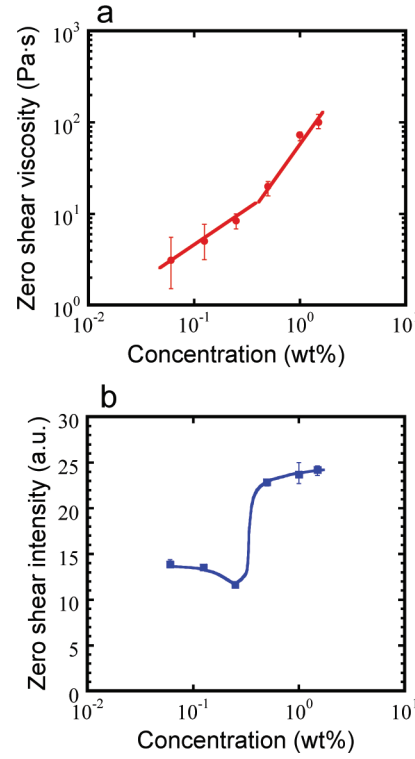

Figure 6. (a) Change in zero shear viscosity for sacran solutions as a function of concentrations. (b) Change in intensity of white light transmitted through sacran solutions under a crossed polarizer as a function of concentrations.

a 10 times increase in shear rate (thixotropy index; Figure S5). The thixotropic effect may be attributed to the interchain sliding of sacran single chains and sacran helixes, which can orient along the shear flow. The high thixotropic value in concentrations higher than 0.5 wt % may be related to the LC state where

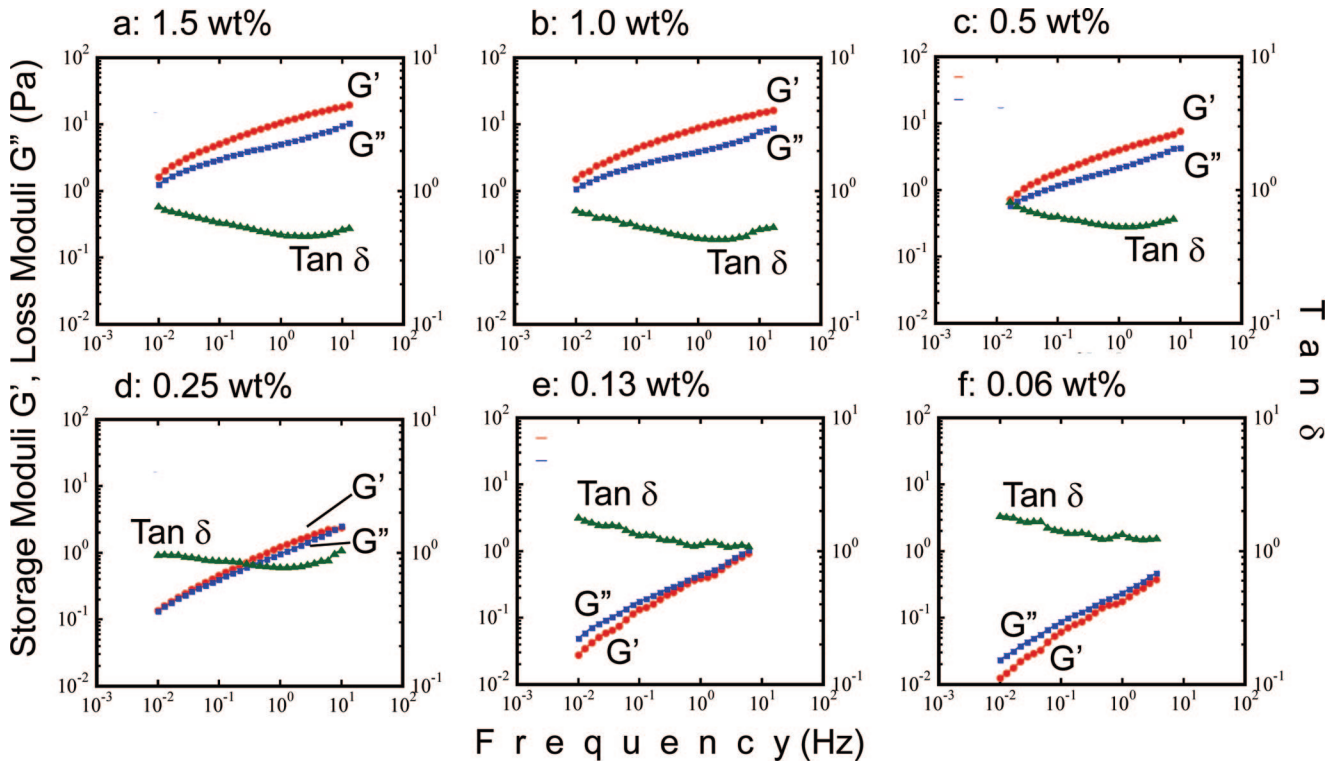

Figure 7. Dynamic moduli for sacran solutions with various concentrations measured at room temperature. In all plots, first and second vertical axes show dynamic moduli and tan δ, respectively, and the horizontal axis shows frequency.

sacran chains orient very smoothly. An increase in the orientation degree of sacran solutions by shear rate increase was confirmed by cross-nicol polarimetry and images of Figure 5c show the intensity increase of light transmitted through sacran solutions with a shear rate increase. The quantitative change in light intensity in Figure 5b shows two-step viscosity increases in sacran solutions in LC states with concentrations of 0.5, 1.0, and 1.5 wt % and an increase in shear rate. The two-step increase was not seen in other polysaccharides such as xantham gum or hyaluronic acid (concentration: 0.5 wt %, Figure S6). The first increase in light intensity occurred in a shear rate range of $10^{-2}-10^{0}$ 1/s while the second increase occurred in a shear rate range of $10^{2}-10^{4}$ 1/s. From the equation of Zimm relaxation time,[22] τ_{Zimm}:

$$\tau_{Zimm} \approx \eta_s R_g^{\,3}/k_B T$$

Where η_s is viscosity, R_g is the mean square radius of polymer chains, k_B is the Boltzmann constant, and T is the absolute temperature, we calculated the R_g scale of sacran chains showing light intensity increases. The first increase occurred in the R_g scale range between 100−300 nm which corresponds with the mean square radius of random-coiled sacran chains (200 nm),[10] while the second increase occurred in the R_g scale between 30−50 nm which was in the same order of helical associates thickness. As a consequence, we can summarize that the first increase in light intensity is attributed to the macroscopic orientation of sacran chains in the LC state while the second light intensity increase is attributed to the extension of sacran chains by strong shear stress.

We measured dynamic moduli of sacran solutions under various concentrations in order to investigate gelation behaviors (Figure 7). Storage moduli, G', of sacran solutions were higher than loss moduli, G'' in concentrations of 0.5, 1.0, and 1.5 wt % while G'' is almost equal to G'' in concentration of 0.25 wt % and is lower than G'' in concentrations of 0.13 and 0.06 wt %. These aforementioned results indicate that sacran solutions adopted a gel state in concentration ranges more than 0.25 wt %. Although the formation mechanism of the cross-linking junction is not clear, we can assume that the bridge formation of double helixes, which is faintly seen in Figure 2c (arrows), may be a driving force for gel formation. Gels were very soft and easily deformed without breaking, suggesting that sacran chains can form double helixes dynamically and interchain interactions may not be very strong.

Discussions

Based on illustrations from Figure 4, we can discuss structural changes in sacran solutions as a function of concentration. Dielectric relaxation studies indicated c^* is 0.02 wt %. In concentration ranges between 0.02−0.09 wt %, sacran chains have a number of opportunities to overlap one another but do not show association behaviors (Figure 4b). Over 0.09 wt %, sacran chains form rigid double helixes (Figure 4c) and this double helix fraction may increase with the concentration. At c = 0.25 wt %, the sacran solution becomes a critical state of sol−gel phase presumably due to an increased fraction of chain entanglement (Figure 4d) and Figure 5b shows a slight increase of the birefringence with shear rate due to the presence of physical cross-linking junctions. The nematic LC phase is exhibited when the concentration exceeds 0.5 wt % (Figure 4e). The concentration showing the LC phase is extremely low because xanthan gum and shizophyllan which are well-known high-performance LC polysaccharides showed an LC phase above 6 wt %[24] and 13 wt %,[25] respectively. Even crystallite rods of charged celluloses with an average length of 115 nm showed a critical LC concentration of 5 wt %.[23] According to the literature,[23,26] electrostatic interactions of mesogenic chains are important to show the LC phase in dilute solutions. The efficient LC formation of sacran chains may be attributed to electrostatic interactions with other polysaccharides and to ultrahigh M_w and lengths of sacran chains, so we calculated the aspect ratio, X, of sacran mesogenic rods from Flory's lattice theory:[27]

$$\varphi = 8/X(1 - 2/X) \approx 8/X$$

Here, ϕ is the volume fraction. When ϕ of the sacran solution is 0.005, X is estimated to be 1600 which is an anomalous value since other LC polysaccharides such as Xanthan gum and shizophyllan show $X = 517$ and $X = 95$, respectively.[21] The thickness of the sacran double helix is estimated to be about 20 nm from Figure 2, and the persistence length of sacran mesogenic chains in the LC state is calculated as 32 μm, which is longer than the calculated and observed length of sacran rods. Sacran mesogenic chains may be derived from the bridged sacran rope and show a LC effect. Thus huge LC domains in centimeter scale are constructed in sacran solution under no external treatments.

Finally we confirmed that the white backlight transmitted through the discolored region during cross-nicol polarimetry (Figure S7) indicated that *A. sacrum* biomaterials show a birefringence. Thus we inferred that the main component of *A. sacrum*, sacran, might be in the LC state *in vivo* and giant rods may reinforce ECMs since the ECM of *A. sacrum* has a water content of 97.5−98.3 wt % ($c = 1.7-2.5\%$). Moreover *A. sacrum* biomaterials show strong laser-light scattering (Figure S9) presumably from sacran rods in the LC state, like LC gels, which are effective upon the dispersion of irradiated light in floating colonies of phototrophic *A. sacrum* cells.

Experimental Section

Materials. Frozen and discolored samples of *A. sacrum* were gifted from Kisendou Inc. (Asakura, Japan) and used as received. Sodium hydroxide (NaOH), ethanol, and 2-propanol, which were used for sacran extraction, were used as received (WAKO pure chemical co. ltd.). Xanthan gum was gifted from Taiyo Kagaku and used as received. Hyaluronic acid sodium salt from *Streptococcus zooepidemicus* was purchased from Sigma and used as received.

Sacran Extraction. We extracted sacran by a procedure shown in the previous reports[9,10] and here show the method simply as follows. After the sample was washed by water and then ethanol, we used NaOH aq for elution of sacran. After some insoluble matters were filtrated, the solution was thoroughly dialyzed with pure water, repeatedly replacing the solution outside of the dialysis membrane (MWCO: 14000). After the solution inside the dialysis membrane was concentrated, it was slowly poured into 2-propanol to create fibrous precipitates, which were reprecipitated twice more to give colorless fibers (inset of Figure 1a).

Measurements. *Viscoelasticity.* Viscoelastic behavior of polysaccharide solutions were measured as follows: A cone plate (25 mm o.d.) was used as a probe for the static rotation viscosity, which was measured at room temperature (approximately 25.0 ± 0.5 °C) by a rotation viscometer (HAAKE MARS2, Ger). The solution thickness was 1 mm (thickness at the center position: 0.053 mm). The probe was prerotated at an angular velocity of 0.01 rpm for 60 s before the measurement was started. The rotation viscosity was recorded with changes in angular velocity from 10^{-3} to 2×10^4 rpm. Zero-shear viscosity was estimated by extrapolation of linear plots to zero velocity. The relative birefringence change of the polysaccharide solution as a function of shear velocity was recorded by measuring the intensity of white light transmitted through the solution (gap: 0.3 mm) under cross-nicol polarimetry. The measurement system included a rheometer with optics, as schematically illustrated in Figure S4. Dynamic viscosity measurements were made by changing the frequency at room temperature using the same systems under static mode.The strain amplitude was set to 10%.

Dielectric Relaxation. The complex dielectric constant ϵ^* of sacran aqueous solutions was measured by an ac two-terminal method using an LCZ meter (HIOKI 3532-50). The frequency ranged from 42 Hz to 5 MHz, and the applied voltage was 0.1 V. The sample cell used in the present study was a coaxial type of cylindrical condenser with stainless-steel electrodes. The dielectric measurement was carried out at room temperature at approximately 25.0 ± 0.5 °C.

Transmission Electron Microscopy (TEM). TEM images were obtained with a Hitachi HF-2000 field emission transmission electron microscope operated at an acceleration voltage of 100 kV at a magnification of 35 000×. The specimens were prepared by slow evaporation of a drop of a diluted MeOH/water (20/1 v/v) solution of sacran (ca. 10 ppm) on a carbon-coated copper mesh grid.

Atomic Force Microscopy (AFM). All AFM experiments were performed using a commercial AFM unit (SPA-400, Seiko Instruments, Japan) equipped with a calibrated 20 μm *xy*-scan and 10 μm *z*-scan range PZT-scanner. For the imaging of sugar chains by AFM, a stiff cantilever (SI-DF20, Seiko Instruments, force constant is 13 N/m in typical value, typical resonant frequency is 130 kHz, pyramidal tip shape, tip curvature radius is 10 nm) were used and imaging was taken in the dynamic force modulation (DFM) mode at optimal force. The scan speed was 2 μm/s.

Acknowledgment. This research was financially supported from a Grant-in-Aid for NEDO (08C46218d) and a Grant-in-Aid from potentiality verification stage of collaborative development of innovative seeds for JST. We acknowledge Kisendou Inc. (Asakura, Japan) for dedicating *A. sacrum* biomaterials.

Supporting Information Available: Figures showing IR spectroscopy and AFM image of sacrans, relaxation time of sacran solution, rheooptics measurement system, light intensity, and polarized and laser-irradiation images of *A. sacrum* biomaterials. This material is available free of charge via the Internet at http://pubs.acs.org.

References and Notes

(1) Gilbert, R. D.; Patton, P. A. *Prog. Polym. Sci.* **1983**, *9*, 115–131.
(2) Greiner, A.; Hou, H.; Reuning, A.; Thomas, A.; Wendorff, J. H.; Zimmermann, S. *Cellulose* **2003**, *10*, 37–52.
(3) Takada, A.; Fujii, K.; Watanabe, J.; Fukuda, T.; Miyamoto, T. *Macromolecules* **1994**, *27*, 1651–1653.
(4) Giraud-Guille, M.-M. *Int. Rev. Cytol.* **1996**, *166*, 59–101.
(5) (a) Vincent, J. F. V. *J. Exp. Biol.* **1999**, *202*, 3263–3268. (b) Mitov, M.; Dessaud, N. *Nat. Mater.* **2006**, *5*, 361–364.
(6) Giraud-Guille, M. M. *Calcified Tissue Int.* **1988**, *42*, 167–180.
(7) Livolant, F. *Phys. A: Stat. Mech. Appl.* **1991**, *176*, 117–137.
(8) Sundaresan, N.; Suresh, C. H.; Thomas, T.; Thomas, T. J.; Pillai, C. K. S. *Biomacromolecules* **2008**, *9*, 1860–1869.
(9) Okajima, M. K.; Ono, M.; Kabata, K.; Kaneko, T. *Pure Appl. Chem.* **2007**, *79*, 2039–2046.
(10) Okajima, M. K.; Bamba, T.; Kaneso, Y.; Hirata, K.; Fukusaki, E.; Kajiyama, S.; Kaneko, T. *Macromolecules* **2008**, *41*, 4061–4064.
(11) Wada, H.; Gombos, Z.; Murata, N. *Nature* **1990**, *347*, 200–203.
(12) Dierking, I. *Textures of Liquid Crystals*; Wiley-VCH Verlag: New York, 2003.
(13) Norisuye, T. *Makromol. Chem. Suppl.* **1985**, *14*, 105–118.
(14) Ferry, J. D.; Oncley, J. L. *J. Am. Chem. Soc.* **1941**, *63*, 272–278.
(15) Cole, K. S.; Cole, R. H. *J. Chem. Phys.* **1941**, *9*, 341–351.
(16) Nagamine, Y.; Ito, K.; Hayakawa, R. *Langmuir* **1999**, *15*, 4135–4138.
(17) Nagamine, Y.; Ito, K.; Hayakawa, R. *Colloid Surf. A Physicochem. Eng. Asp.* **1999**, *148*, 149–153.
(18) Mandel, M. *Mol. Phys.* **1961**, *4*, 489–496.
(19) Sakamoto, M.; Kanda, H.; Hayakawa, R.; Wada, Y. *Biopolymers* **1976**, *15*, 879–892.
(20) Mitsumata, T.; Ikeda, K.; Gong, J. P.; Osada, Y. *J. Phys. Chem.* **1998**, *102*, 5246–5251.
(21) De Gennes, P. G. *Physics of Liquid Crystals*; Oxford Univ. Press: Oxford, U.K., 1995.
(22) Doi, M.; Edwards, S. F. *The Theory of Polymer Dynamics*; Clarendon: Oxford, U.K., 1986.
(23) Oertel, R.; Kulicke, W. M. *Rheol. Acta* **1991**, *30*, 140–150.
(24) Van, K.; Norisuye, T.; Teramoto, A. *Mol. Cryst. Liq. Cryst.* **1981**, *78*, 123–124.
(25) Dong, X. M.; Gray, D. G. *Langmuir* **1997**, *13*, 2404–2409.
(26) Teramoto, A.; Sato, T. *Lect. Notes Phys.* **1993**, *415*, 399–410.
(27) (a) Flory, P. J. *Proc. R. Soc. London, A* **1956**, *234*, 73–89. (b) Flory, P. J. *Adv. Polym. Sci.* **1984**, *59*, 1–36.

MA802829X